Inorganic Chemistry

Article

pubs.acs.org/IC

Mercury- and Cadmium-Assisted [2 + 2] Cyclodimerization of *tert*-Butylselenium Diimide

Aino J. Karhu,[†] J. Mikko Rautiainen,[†] Raija Oilunkaniemi,[†] Tristram Chivers,[‡] and Risto S. Laitinen*[,†]

[†]Laboratory of Inorganic Chemistry, Center for Molecular Materials, University of Oulu, P.O. Box 3000, FI-90014 Oulu, Finland

[‡]Department of Chemistry, University of Calgary, 2500 University Drive NW, Calgary, Alberta T2N 1N4, Canada

Supporting Information

ABSTRACT: The complexes $[MCl_2\{N,N'\text{-}^tBuNSe(\mu\text{-}N^tBu)_2SeN^tBu\}]$ [M = Cd (**1**), Hg (**2**)] were obtained in high yields by the reaction of *tert*-butylselenium diimide $Se^{IV}(N^tBu)_2$ with $CdCl_2$ or $HgCl_2$ in tetrahydrofuran. Recrystallization of **1** and **2** from acetonitrile (MeCN) afforded yellow crystals of **1**·MeCN and **2**·MeCN, respectively. Isomorphic **1**·MeCN and **2**·MeCN contain an unprecedented dimeric selenium diimide ligand, which is N,N′-chelated to the metal through exocyclic imido groups. In addition to the complexes **1** and **2**, the ^{77}Se NMR spectra of acetonitrile solutions of **1**·MeCN and **2**·MeCN indicated the presence of the dimeric $^tBuNSe(\mu\text{-}N^tBu)_2SeN^tBu$, monomeric $Se^{IV}(N^tBu)_2$, and cyclic selenium imides. Density functional theory calculations at the PBE0/def2-TZVPP level of theory were used to assign the ^{77}Se resonances of the dimer. A comparison of Gibbs energies of formation of some metal dichloride complexes $[MCl_2\{N,N'\text{-}Se^{IV}(N^tBu)_2\}]$ and $[MCl_2\{N,N'\text{-}^tBuNSe(\mu\text{-}N^tBu)_2SeN^tBu\}]$ (M = Zn, Cd, Hg) indicated that the formation of complexes containing a dimeric selenium diimide ligand is favored over those containing a monomeric ligand for the group 12 metals. In the case of the group 10 metal halogenides (M = Ni, Pd, Pt), the Gibbs energies of the complexes with monomeric $Se^{IV}(N^tBu)_2$ ligands are close to those containing dimeric $^tBuNSe(\mu\text{-}N^tBu)_2SeN^tBu$ ligands. A plausible reaction pathway with a low activation energy involves the initial formation of $[MCl_2\{N,N'\text{-}Se^{IV}(N^tBu)_2\}]$ (M = Zn, Cd, Hg), which then reacts with another molecule of $Se(N^tBu)_2$, leading to the final $[MCl_2\{N,N'\text{-}^tBuNSe(\mu\text{-}N^tBu)_2SeN^tBu\}]$ complex. Without the presence of group 12 metal halogenides, the [2 + 2] cyclodimerization of $Se^{IV}(N^tBu)_2$ is virtually thermoneutral, but the activation energy is relatively high, which accounts for the kinetic stability of $^tBuNSe(\mu\text{-}N^tBu)_2SeN^tBu$ in solution. A minor byproduct, $[Cd_7Cl_{14}\{N,N'\text{-}Se^{II}(NH^tBu)_2\}_6]\cdot 4CH_2Cl_2$, was identified by X-ray crystallography as a heptanuclear cluster with selenium(II) diamide ligands N,N′-chelated to the cadmium centers.

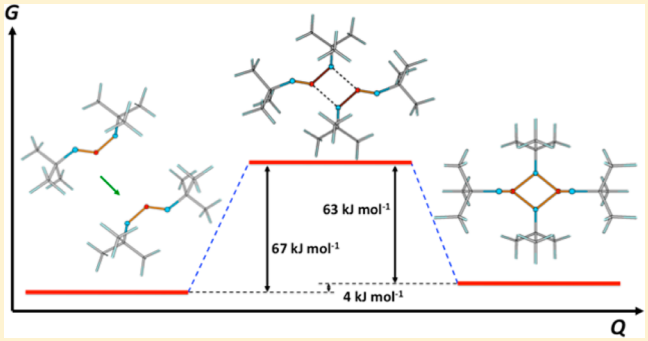

INTRODUCTION

Chalcogen diimides RN═E═NR (E = S, Se, Te; R = alkyl or aryl group), as well as chalcogen dioxides and imide oxides, exhibit an increasing reluctance for the heavier chalcogen elements to engage in multiple bonds (see Chart 1).[1] This is a consequence of the highly polar nature of E−N and E−O bonds as well as their reluctance to engage pπ−pπ multiple bonds.[2] While sulfur diimides are stable monomeric compounds, selenium diimides are thermally unstable, decomposing to give a mixture of cyclic selenium imides.[3] The corresponding tellurium diimides are thermally stable dimers as a consequence of facile [2 + 2] cyclodimerization, as exemplified by *tert*-butyltellurium diimide.[4] A similar trend is observed for heteroleptic imide oxides (see Chart 1).[5]

Consistent with experimental observations, density functional theory (DFT) calculations of the energies of the cyclodimerization $E(NR)_2$ to form the corresponding dimers $RNE(\mu\text{-}NR)_2ENR$ (E = S, Se, Te; R = H, Me, ^{t}Bu, $SiMe_3$; see Scheme 1) revealed that the process is clearly endothermic for sulfur diimides, approximately thermoneutral for selenium diimides, and strongly exothermic for tellurium diimides.[3f,5d,6] The related [2 + 2] cyclodimerization of ^{t}BuNSeO to give $OSe(\mu\text{-}N^tBu)_2SeO$[5c] and the cycloaddition of $Se(N^tBu)_2$ with $^tBuNEO_x$ (E = S, x = 2; E = Se, x = 1) to produce $^tBuNSe(\mu\text{-}N^tBu)_2SO_2$ or $^tBuNSe(\mu\text{-}N^tBu)_2SeO$,[3e] respectively, are also energetically favorable processes.[3f]

Monomeric sulfur diimides can adopt three possible conformations (see Chart 2). With the exception of the parent $S(NH)_2$ and some aromatic derivatives, for which the cis,cis conformation (**1A**) is most stable,[7] the cis,trans conformation (**1B**) is observed for most diimides.[1] The trans,trans conformation (**1C**) is found at higher relative energy. The structural information for selenium diimides is much sparser. The solution ^1H and ^{13}C NMR spectra of $Se(N^tBu)_2$ have been interpreted in terms of the cis,trans conformation (**1B**).[3d] The

Received: June 25, 2015
Published: September 17, 2015

DOI: 10.1021/acs.inorgchem.5b01434
Inorg. Chem. 2015, 54, 9499−9508

Chart 1. Tendency of Chalcogen Imides and Oxides To Form Dimers and Polymers

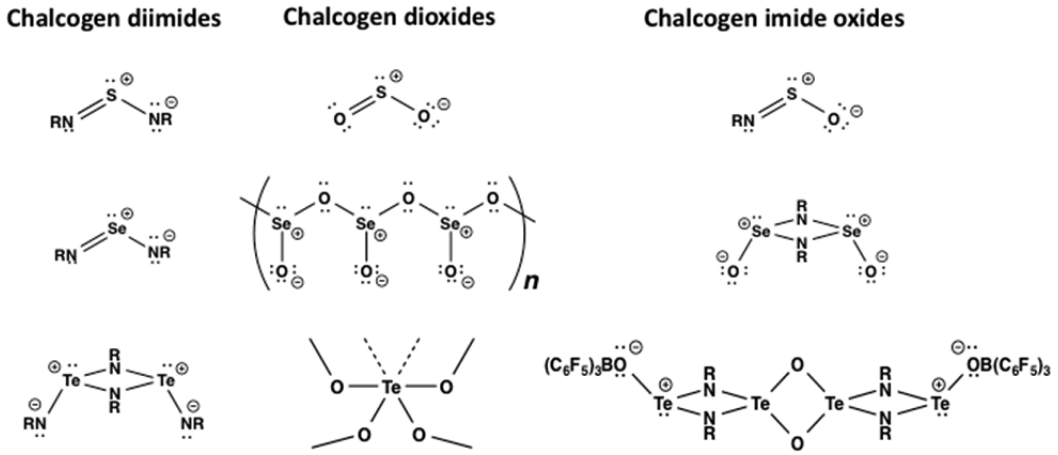

Scheme 1. [2 + 2] Cyclodimerization of Chalcogen Diimides

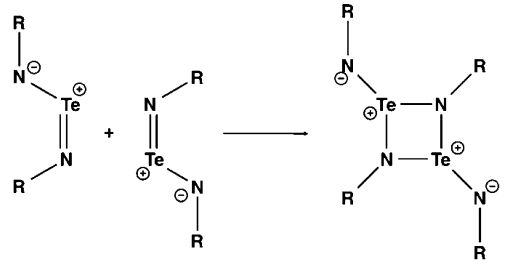

Chart 2. Possible Conformations of $E(NR)_2$ Monomers (1A–1C) and $RNE(\mu\text{-}NR)_2ENR$ Dimers (2A–2E)[a]

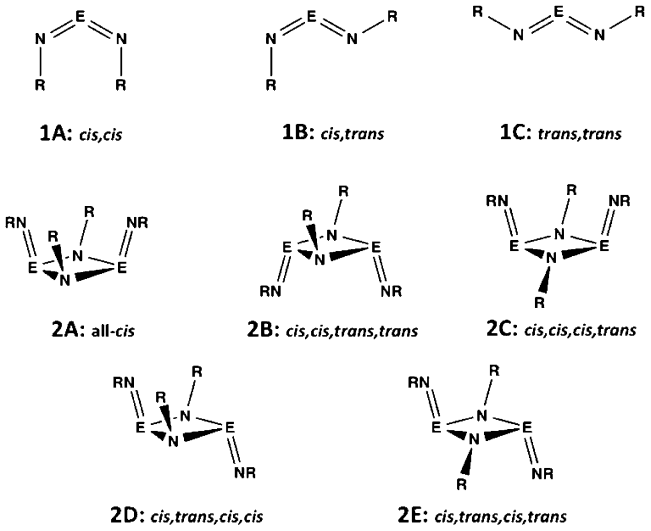

[a]The first two structural descriptors refer to exocyclic NR groups, while the latter two indicate endocyclic NR groups (for simplicity, polar contributions to the E = NR bonds are not shown).

X-ray structure of adamantylselenium diimide also shows the monomeric cis,trans conformation.[5c] However, the bulky supermesityl groups in $Se\{N(mes^*)\}_2$ appear to enforce the trans,trans conformation in both the solid state and solution.[8] In the case of $Se(NSiMe_3)_2$, there are some indications that this selenium diimide may be dimeric in solution.[3c,9]

Dimeric chalcogen diimides can also adopt several conformations (see Chart 2). DFT calculations have indicated that the all-cis arrangement (**2A**) is energetically most favorable.[3f] Experimental information is restricted to the *tert*-butyltellurium diimide dimer ^{t}BuNTeN(μ-N^{t}Bu)$_2$TeN^{t}Bu, which exists in the cis,cis,trans,trans conformation (**2B**) in the solid state with both exocyclic R groups in endo conformations.[4b] The arrangement **2B** with the exocyclic R groups in exo conformations is observed for the unsymmetrical derivatives RTeN(μ-NR′)$_2$TeNR (R = PPh_2NSiMe_3; R′ = ^{t}Bu, ^{t}Oct) in the solid state.[4a,c]

Chalcogen diimides are attractive ligands because of the availability of three potential donor sites and two formal π bonds.[1] The coordination chemistry of sulfur diimides is particularly rich.[10] Several different bonding modes are known depending both on of the nature of the metal center and on the steric and electronic properties of the diimide ligand;[11] however, N,N′-chelation is commonly observed for both transition-metal and main-group-metal complexes.[11b−f]

Although investigations of the coordination behavior of monomeric selenium diimides are limited by their thermal instability (vide infra),[3] it has been established that they can act as either chelating or bridging ligands in metal complexes.[1c] For example, $Se(N^tBu)_2$ forms mononuclear N,N′-chelated complexes with $SnCl_4$,[11e] $PdCl_2$,[11f] and $PtCl_2$.[12] In these complexes, the selenium diimide ligand is forced to adopt the energetically less favorable trans,trans configuration. The bridging N,N′-coordination mode is found in the dinuclear coinage metal complexes $[M_2\{\mu\text{-}N,N'\text{-}Se(NR)_2\}_2]^{2+}$ (M = Cu, Ag; R = ^{t}Bu, Ad) in which the ligands bridge an $[M\cdots M]^{2+}$ unit.[13] The tellurium diimide dimer ^{t}BuNTe(μ-N^{t}Bu)$_2$TeN^{t}Bu forms an analogous N,N′-chelated complex with an $[Ag\cdots Ag]^{2+}$ moiety, but the corresponding copper complex has an open-chain structure in which one tellurium diimide dimer acts as a bridging ligand between single metal centers.[14] The dimer ^{t}BuNTe(μ-N^{t}Bu)$_2$TeN^{t}Bu also forms N,N′-chelated complexes with single metal centers, e.g., [MCl$_2${*N*,*N*′-^{t}BuNTe(μ-N^{t}Bu)$_2$TeN^{t}Bu}] (M = Co,[15] Hg[16]).

In the context of the foregoing background and, in particular, in view of the thermoneutrality of the dimerization process for selenium diimides, we were interested in determining whether a metal center could induce the dimerization process during the complex formation. With this in mind, we have explored the reactions of $Se(N^tBu)_2$ with the group 12 halogenides $CdCl_2$ and $HgCl_2$, which afforded complexes of the selenium diimide dimer [MCl$_2${*N*,*N*′-^{t}BuNSe(μ-N^{t}Bu)$_2$SeN^{t}Bu}] [M = Cd (**1**), Hg (**2**)] in excellent yields. This interesting finding represents

DOI: 10.1021/acs.inorgchem.5b01434
Inorg. Chem. 2015, 54, 9499−9508

Table 1. Crystal Data and Details of the Structure Determinations of 1·MeCN, 2·MeCN, and 3·4CH_2Cl_2

	1·MeCN	2·MeCN	3·4CH_2Cl_2
empirical formula	$C_{18}H_{39}CdCl_2N_5Se_2$	$C_{18}H_{39}HgCl_2N_5Se_2$	$C_{52}H_{128}Cd_7Cl_{22}N_{12}Se_6$
fw	666.76	754.95	2962.12
temperature (K)	150	150	150
cryst syst	orthorhombic	orthorhombic	triclinic
space group	*Pbca*	*Pbca*	$P\bar{1}$
a (Å)	18.468(5)	18.485(5)	13.821(5)
b (Å)	14.827(5)	14.886(5)	14.266(5)
c (Å)	20.426(5)	20.405(5)	16.301(5)
α (deg)			65.554(5)
β (deg)			85.791(5)
γ (deg)			62.335(5)
V (Å^3)	5593(3)	5615(3)	2563.2(15)
Z	8	8	1
F(000)	2656	2912	1438
D_c (g cm^{-3})	1.584	1.786	1.919
μ(Mo K*α*) (mm^{-1})	3.588	8.279	4.165
cryst size (mm)	0.20 × 0.15 × 0.10	0.40 × 0.10 × 0.10	0.20 × 0.10 × 0.05
indep/obsd reflns[a]	5494/4585	5510/4431	9973/8535
R_{int}	0.1154	0.1308	0.0682
R1/wR2 [$I \geq 2\sigma(I)$][a]	0.0386/0.0945	0.0471/0.1101	0.0427/0.0965
R1/wR2 (all data)[b]	0.0532/0.1026	0.0670/0.1204	0.0551/0.1034
GOF	1.103	1.129	1.102

[a] $R1 = \sum||F_o| - |F_c||/\sum|F_o|$. [b] $wR2 = [\sum w(F_o^2 - F_c^2)^2/\sum wF_o^4]^{1/2}$.

the first observation of the [2 + 2] cyclodimerization of a selenium diimide. The energetics of the dimerization process in the presence of various metal dihalogenides have been investigated by DFT calculations. The X-ray structure of the heptanuclear $[Cd_7Cl_{14}\{N,N'\text{-}Se(NH^tBu)_2\}_6]$ (**3**), a minor byproduct from the $CdCl_2$ reaction, is also discussed.

EXPERIMENTAL SECTION

General Procedures. All reactions and manipulations of air- and moisture-sensitive products were carried out under an argon atmosphere by using a standard drybox or Schlenk technique. Tetrahydrofuran (THF) and diethyl ether were dried by distillation over sodium/benzophenone, and acetonitrile was dried over CaH_2 under an argon atmosphere prior to use. $SeCl_4$ (Strem Chemicals), $CdCl_2$ (Strem Chemicals), and $HgCl_2$ (Merck) were used as purchased. $^tBuNH_2$ (Aldrich) was distilled over KOH and stored over molecular sieves. *tert*-Butylselenium diimide $Se(N^tBu)_2$ was prepared from $SeCl_4$ and $^tBuNH_2$, as described by Herberhold and Jellen,[3b] and kept at 0 °C at all times to reduce decomposition.

NMR Spectroscopy. The ^{77}Se and ^{199}Hg NMR spectra were recorded in a CH_3CN/CD_3CN solution (2:5) on a Bruker Avance III 400 spectrometer operating at 76.31 and 71.67 MHz, respectively. The spectra were recorded unlocked. Typical respective spectral widths for ^{77}Se and ^{199}Hg were 113.64 and 71.43 kHz, and the pulse widths were 16.75 and 6.00 μs. The pulse delay for both selenium and mercury was 1.0 s. A saturated D_2O solution of SeO_2 and a 1.0 M solution of $HgCl_2$ in dimethyl sulfoxide (DMSO)-d_6 were used as external standards for ^{77}Se and ^{199}Hg chemical shifts, respectively. The ^{77}Se and ^{199}Hg chemical shifts are reported relative to neat Me_2Se [$\delta(Me_2Se) = \delta(SeO_2) + 1302.6$][17] and to neat Me_2Hg [$\delta(Me_2Hg) = \delta(HgCl_2$, 1 M in DMSO-$d_6$) − 1501.6].[18]

*Preparation of [$CdCl_2$\{N,N′-^{t}BuNSe(μ-N^{t}Bu)$_2$SeN^{t}Bu\}] (**1**).* A yellow solution of $Se(N^tBu)_2$ (0.477 g, 2.16 mmol) in THF (10 mL) was added dropwise to a stirred white slurry of $CdCl_2$ (0.180 g, 0.98 mmol) in THF (15 mL) at −80 °C. After 1 h at −80 °C, the reaction mixture was warmed slowly to room temperature and stirred overnight to give a yellow solution and a yellow precipitate. The solvent was removed under vacuum, and the solid residue was extracted with acetonitrile (5 × 10 mL). After filtration, the solvent was removed from the combined extracts under vacuum to give **1** as a yellow solid (0.504 g, 0.805 mmol; yield 82% based on $CdCl_2$). Anal. Calcd for $C_{16}H_{36}Cl_2CdN_4Se_2$ (**1**): C, 30.71; H, 5.80; N, 8.95. Found: C, 29.78; H, 5.82; N, 8.34. ^{77}Se NMR (CH_3CN/CD_3CN): *δ* 1080. Yellow crystals of **1**·MeCN suitable for the X-ray structure determination were obtained by recrystallization from acetonitrile at −20 °C. Anal. Calcd for $C_{18}H_{39}Cl_2CdN_5Se_2$ (**1**·MeCN): C, 32.42; H, 5.90; N, 10.50. Found: C, 31.92; H, 5.92; N, 10.39.

A few colorless crystals of **3** were obtained in one reaction. X-ray-quality crystals of the solvate 3·4CH_2Cl_2 were obtained by recrystallization of this byproduct from dichloromethane followed by manual separation.

*Preparation of [$HgCl_2$\{N,N′-^{t}BuNSe(μ-N^{t}Bu)$_2$SeN^{t}Bu\}] (**2**).* A THF (10 mL) solution of $Se(N^tBu)_2$ (0.524 g, 2.37 mmol) was added dropwise to a stirred colorless solution of $HgCl_2$ (0.293 g, 1.08 mmol) in THF (15 mL) at −80 °C. After 1 h at −80 °C, the reaction mixture was warmed slowly to room temperature and stirred overnight to give a yellow solution. The solvent was removed under vacuum, and the solid residue was extracted with acetonitrile (4 × 10 mL). After filtration, the solvent was removed from the combined extracts under vacuum to give **2** as a yellow solid (0.609 g, 0.853 mmol; yield 79% based on $HgCl_2$). Anal. Calcd for $C_{16}H_{36}Cl_2HgN_4Se_2$ (**2**): C, 26.92; H, 5.08; N, 7.85. Found: C, 27.14; H, 5.23; N, 7.67. ^{77}Se NMR (CH_3CN): *δ* 1093. ^{199}Hg NMR (CH_3CN): *δ* −1190. Yellow crystals of **2**·MeCN suitable for the X-ray structure determination were obtained by recrystallization from acetonitrile at −20 °C. Anal. Calcd for $C_{18}H_{39}Cl_2HgN_5Se_2$ (**2**·MeCN): C, 28.64; H, 5.21; N, 9.28. Found: C, 28.63; H, 5.21; N, 9.31.

X-ray Crystallography. Diffraction data for compounds **1**·MeCN, **2**·MeCN, and 3·4CH_2Cl_2 were collected on a Nonius Kappa CCD diffractometer at 150 K using graphite-monochromated Mo K*α* radiation (*λ* = 0.71073 Å; 55 kV, 25 mA). Crystal data and the details of structure determinations are given in Table 1. All structures were solved by direct methods using *SHELXS-2013* and refined using *SHELXL-2013*.[19] After the full-matrix least-squares refinement of the non-hydrogen atoms with anisotropic thermal parameters, the hydrogen atoms were placed in calculated positions in the methyl groups (C−H = 0.98 Å). The hydrogen atoms bound to nitrogen in 3·4CH_2Cl_2 were located in the difference Fourier map. In the final refinement, all methyl hydrogen atoms were placed at calculated

DOI: 10.1021/acs.inorgchem.5b01434
Inorg. Chem. 2015, 54, 9499−9508

positions and were riding with the atoms they were bonded to. The hydrogen atoms bound to nitrogen were refined independently. The isotropic thermal parameters of the hydrogen atoms were fixed at 1.5 times that of the corresponding carbon or nitrogen. The scattering factors for the neutral atoms were those incorporated with the program.

COMPUTATIONAL DETAILS

All calculations were performed on the *Gaussian 09* program.[20] Calculations employed the PBE0 hybrid functional[21] and def2-TZVPP basis sets,[22] as implemented in *Gaussian 09*. Dispersion forces were treated in the calculations by using the D3BJ version of Grimme's empirical correction with Becke–Johnson damping parametrized for the PBE0 functional.[23] Full geometry optimization was carried out for each species considered in this work. Energies in THF were calculated using the CPCM method implemented in *Gaussian 09*.[24] Nuclear magnetic shielding tensors were calculated using the GIAO method[25] for each stationary point.

RESULTS AND DISCUSSION

Syntheses. The reactions of 2 equiv of monomeric $Se(N^tBu)_2$ with 1 equiv of $CdCl_2$ or $HgCl_2$ afforded excellent yields of the air- and moisture-sensitive solids **1** and **2**, respectively (eq 1), which were recrystallized from acetonitrile as **1**·MeCN and **2**·MeCN.

$$2Se(N^tBu)_2 + MCl_2 \rightarrow [MCl_2\{N,N'\text{-}{}^t\text{BuNSe}(\mu\text{-}N^tBu)_2SeN^tBu\}]_{\mathbf{1},M=Cd;\mathbf{2},M=Hg} \quad (1)$$

Concomitant with the formation of **1**, a few colorless crystals were isolated from one reaction and subsequently identified as $3{\cdot}4CH_2Cl_2$ by a single-crystal X-ray structure determination (vide infra).

*Crystal Structures of [MCl_2\{N,N′-^{t}BuNSe(μ-N^{t}Bu)$_2$SeN^{t}Bu\}]·MeCN [M = Cd (**1**), Hg (**2**)].* The molecular structures of **1**·MeCN and **2**·MeCN are shown, together with the atomic numbering scheme in Figure 1. Selected bond parameters are summarized in Table 2. The structures of **1**·MeCN and **2**·MeCN are isomorphic and consist of the selenium diimide dimer ^{t}BuNSe(μ-N^{t}Bu)$_2$SeN^{t}Bu N,N′-chelated to the metal center through exocyclic nitrogen atoms. The complexes **1**·MeCN and **2**·MeCN are isostructural with the mercury and cobalt complexes of the corresponding tellurium diimide dimer $[HgCl_2\{N,N'\text{-}{}^t\text{BuNTe}(\mu\text{-}N^tBu)_2TeN^tBu\}]{\cdot}MeCN$[16] and $[CoCl_2\{N,N'\text{-}{}^t\text{BuNTe}(\mu\text{-}N^tBu)_2TeN^tBu\}]{\cdot}CH_2Cl_2$,[15] respectively. The metal centers in **1**·MeCN and **2**·MeCN adopt tetrahedral coordination with bond angles in the ranges 107.75(9)–112.63(13)° and 107.18(16)–110.61(7)°, respectively.

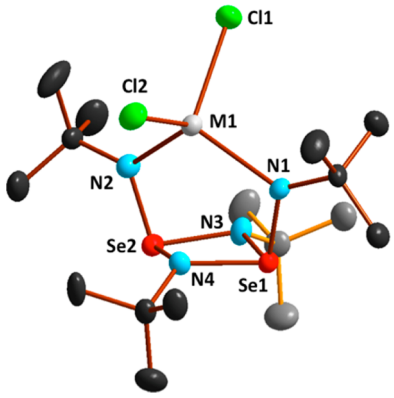

Figure 1. Molecular structure of $[MCl_2\{N,N'\text{-}{}^t\text{BuNSe}(\mu\text{-}N^tBu)_2SeN^tBu\}]$ [M = Cd (**1**), Hg (**2**)] indicating the numbering of the atoms. The thermal ellipsoids have been drawn at the 50% probability level. Hydrogen atoms have been omitted for clarity.

In both **1**·MeCN and **2**·MeCN, the chelating ^{t}BuNSe(μ-N^{t}Bu)$_2$SeN^{t}Bu ligand exhibits the **2B** conformation (see Chart 2) with the exocyclic *tert*-butyl groups in the exo conformation (see Figure 1), as was found in the aforementioned MCl_2 (M = Hg, Co) complexes of ^{t}BuNTe(μ-N^{t}Bu)$_2$TeN^{t}Bu.[15,16] The Se_2N_2 ring in both **1**·MeCN and **2**·MeCN is slightly puckered, displaying the angles between the planes N3–Se1–N4 and N3–Se2–N4 of 169.06(14) and 171.4(2)°, respectively. The geometry at the bridging nitrogen atoms N3 and N4 deviates significantly from planarity [$\sum\angle$(N3) = 345.4° and 346.4° and $\sum\angle$(N4) = 346.4° and 349.1° in **1**·MeCN and **2**·MeCN, respectively]. The endocyclic Se–N bonds of the Se_2N_2 ring in **1**·MeCN and **2**·MeCN span the ranges 1.881(3)–1.892(4) and 1.874(6)–1.886(6) Å, respectively, compared to a typical Se–N single bond length of 1.87 Å[26] and endocyclic Se–N bond distances of 1.881(2)–1.888(2) Å in OSe(μ-N^{t}Bu)$_2$SeO[5c] and 1.862(4)–1.943(4) Å in ^{t}BuNSe(μ-N^{t}Bu)$_2$SeO.[3e]

The exocyclic Se–N bond lengths in **1**·MeCN [1.724(3) and 1.735(4) Å] and in **2**·MeCN [1.711(6) and 1.728(5) Å] indicate double-bond character, compared to 1.710(3) Å in $[SnCl_4\{N,N'\text{-}Se(N^tBu)_2\}]$[11e] and 1.731(4)–1.736(4) Å in $[PdCl_2\{N,N'\text{-}Se(N^tBu)_2\}]$.[11f] The geometry at the exocyclic nitrogen atoms N1 and N2 is planar [$\sum\angle$(N1,N2) = 360.0 and 359.9° and also 360.0° for **1**·MeCN and **2**·MeCN, respectively].

The MeCN molecule in the lattice interacts with a chlorine atom of **1** and **2** via H···Cl hydrogen bonds of 2.6667(13) and 2.730(2) Å, respectively. Both complexes are also linked by additional weak Cl···H hydrogen bonds [**1**, Cl1···H41A = 2.8408(14) Å, Cl2···H13C = 2.9028(13) Å, and Cl2···H32C = 2.9096(13) Å; **2**, Cl1···H41A = 2.836(2) Å, Cl2···H13C = 2.874(2) Å, and Cl2···H32C = 2.904(2) Å].

Optimized Structures of [MCl_2\{N,N′-Se(N^{t}Bu)$_2$\}] and [MCl_2\{N,N′-^{t}BuNSe(μ-N^{t}Bu)$_2$SeN^{t}Bu\}] (M = Zn, Cd, Hg, Ni, Pd, Pt). The cyclodimerization of $Se(N^tBu)_2$ upon the formation of **1**·MeCN and **2**·MeCN raised an obvious question about the stability of the dimer. In order to discuss the energetics of the dimerization process and the complex formation, the optimized PBE0/def2-TZVPP geometries of $Se(N^tBu)_2$, ^{t}BuNSe(μ-N^{t}Bu)$_2$SeN^{t}Bu, and complexes **1** and **2**, together with some related selenium diimide complexes, were calculated. As indicated in Table 3, there is a good agreement between the calculated and experimental bond parameters. The discussion of the geometry optimization of all species together with the *xyz* files of the optimized structures is presented in the Supporting Information.

^{77}Se NMR Spectra. The ^{77}Se NMR spectra of the reaction mixtures of MCl_2 (M = Cd, Hg) and $Se(N^tBu)_2$ in THF indicated the presence of the reagent $Se(N^tBu)_2$ (δ 1654),[3d] together with its known decomposition products $Se_3(N^tBu)_3$ (δ 1396) and $Se_3(N^tBu)_2$ (δ 1626 and 1183; intensity ratio 1:2),[3e] as well as OSe(μ-N^{t}Bu)$_2$SeO (δ 1242),[3f] reflecting the use of a slight excess of $Se(N^tBu)_2$ in these reactions. The spectra also showed a relatively strong resonance at 1149 ppm, which has not been previously observed among the decomposition products of $Se(NR)_2$ (R = ^{t}Bu, adamantyl) in a THF solution.[3e,f]

DOI: 10.1021/acs.inorgchem.5b01434
Inorg. Chem. 2015, 54, 9499–9508

Table 2. Selected Bond Lengths (Å) and Angles (deg) in 1·MeCN and 2·MeCN

	1·MeCN	2·MeCN		1·MeCN	2·MeCN
M1−Cl1	2.4521(12)	2.460(2)	Se2−N2	1.735(4)	1.711(6)
M1−Cl2	2.4492(12)	2.469(2)	Se2−N3	1.885(4)	1.874(6)
M1−N1	2.302(3)	2.326(5)	Se2−N4	1.886(3)	1.875(6)
M1−N2	2.287(3)	2.320(6)	N1−C1	1.478(6)	1.475(9)
Se1−N1	1.724(3)	1.728(5)	N2−C2	1.484(5)	1.511(9)
Se1−N3	1.892(4)	1.885(6)	N3−C3	1.492(5)	1.483(9)
Se1−N4	1.881(3)	1.886(6)	N4−C4	1.502(5)	1.478(9)
Cl1−M1−Cl2	109.30(5)	110.61(7)	N1−Se1−N3	98.83(17)	99.0(3)
Cl1−M1−N1	107.91(10)	109.97(16)	N1−Se1−N4	95.66(16)	97.2(3)
Cl1−M1−N2	108.53(10)	110.05(16)	N3−Se1−N4	78.17(15)	78.3(3)
Cl2−M1−N1	107.75(9)	107.18(16)	N2−Se2−N3	99.39(17)	100.0(3)
Cl2−M1−N2	110.65(10)	109.15(16)	N2−Se2−N4	96.21(15)	97.3(3)
N1−M1−N2	112.63(13)	109.8(2)	N3−Se2−N4	78.20(15)	78.8(3)

Table 3. Bond Distances of PBE0/def2-TZVPP-Optimized Structures of $[MCl_2\{N,N'\text{-}Se(N^tBu)_2\}]$ and $[MCl_2\{N,N'\text{-}^tBuNSe(\mu\text{-}N^tBu)_2SeN^tBu\}]$ (M = Zn, Cd, Hg, Ni, Pd, Pt)

	PBE0/def2-TZVPP (Å)			experimental bond lengths (Å)			
compound	M−N	M−Cl	N−Se	M−N[a]	M−Cl[a]	N−Se[a]	ref[b]
$^tBuNSe(\mu\text{-}N^tBu)_2SeN^tBu$ (all-cis, C_{2v})			1.695/1.862				
$Se(N^tBu)_2$ (cis,trans, C_s)			1.681/1.704			1.679/1.732[c]	5c
$[ZnCl_2\{N,N'\text{-}^tBuNSe(\mu\text{-}N^tBu)_2SeN^tBu\}]$ (C_1)[d]	2.135	2.239	1.710/1.852				
$[ZnCl_2\{N,N'\text{-}Se(N^tBu)_2\}]$ (C_{2v})	2.198	2.179	1.696				
$[CdCl_2\{N,N'\text{-}^tBuNSe(\mu\text{-}N^tBu)_2SeN^tBu\}]$ (C_{2v})	2.379	2.403	1.700/1.851	2.294	2.451	1.729/1.886	this work
$[CdCl_2\{N,N'\text{-}Se(N^tBu)_2\}]$ (C_{2v})	2.451	2.346	1.694				
$[HgCl_2\{N,N'\text{-}^tBuNSe(\mu\text{-}N^tBu)_2SeN^tBu\}]$ (C_{2v})	2.569	2.360	1.696/1.854	2.323	2.464	1.719/1.880	this work
$[HgCl_2\{N,N'\text{-}Se(N^tBu)_2\}]$ (C_{2v})	2.718	2.303	1.691				
$[NiCl_2\{N,N'\text{-}^tBuNSe(\mu\text{-}N^tBu)_2SeN^tBu\}]$ (C_2)[e]	1.993	2.175	1.721/1.848				
$[NiCl_2\{N,N'\text{-}Se(N^tBu)_2\}]$ (C_{2v})	1.949	2.130	1.716				
$[PdCl_2\{N,N'\text{-}^tBuNSe(\mu\text{-}N^tBu)_2SeN^tBu\}]$ (C_s)	2.148	2.282	1.723				
$[PdCl_2\{N,N'\text{-}Se(N^tBu)_2\}]$ (C_{2v})	2.050	2.247	1.721	2.050	2.284	1.733	11f
$[PtCl_2\{N,N'\text{-}^tBuNSe(\mu\text{-}N^tBu)_2SeN^tBu\}]$ (C_s)	2.092	2.294	1.734				
$[PtCl_2\{N,N'\text{-}Se(N^tBu)_2\}]$ (C_{2v})	2.008	2.263	1.741	2.024	2.290	1.748	12

[a]Average values, as appropriate. [b]The references cite experimental values. [c]Adamantylselenium diimide $Se(NAd)_2$. [d]The symmetric C_{2v} structure had two negative frequencies. The true minimum had C_1 symmetry. The values shown in the table are average values. [e]The symmetric C_{2v} structure had one negative frequency. The true minimum had C_2 symmetry. The values shown in the table are average values.

The ^{77}Se NMR spectrum of crystals of **1**·MeCN dissolved in CH_3CN/CD_3CN revealed the presence of the cyclic selenium imides $Se_3(N^tBu)_3$ and $Se_3(N^tBu)_2$,[3e] in addition to previously unobserved resonances at 1080 and 1219 ppm (see Figure 2a). The latter resonance was also present in the ^{77}Se NMR spectrum of **2**·MeCN redissolved in CH_3CN/CD_3CN, in addition to the resonance at 1093 ppm and a resonance for $Se(N^tBu)_2$ at δ 1666 ppm (see Figure 2b). When the resonances for $Se(N^tBu)_2$ (Figure 2b) and its decomposition products are disregarded (Figure 2a), the ^{77}Se NMR spectra of **1** and **2** differ from each other only with respect to one resonance. Thus, the resonance at 1080 ppm in Figure 2a can be attributed to complex **1** and that at 1093 ppm in Figure 2b to **2**.

The resonance at 1219 ppm, which is observed in the spectra of both **1**·MeCN and **2**·MeCN in the CH_3CN/CD_3CN solution, can be assigned to the dimer $^tBuNSe(\mu\text{-}N^tBu)_2SeN^tBu$; the resonance at 1149 ppm observed in THF solutions of the reaction mixtures (vide supra) may also be due to this dimer. We note for comparison that the analogous tellurium diimide dimer $^tBuNTe(\mu\text{-}N^tBu)_2TeN^tBu$ exhibits a ^{125}Te NMR resonance in toluene at 1476 ppm.[4b,d] This resonance bears a reasonable qualitative relationship with the ^{77}Se chemical shift of 1219 ppm assigned to $^tBuNSe(\mu\text{-}N^tBu)_2SeN^tBu$.[27]

Calculated ^{77}Se NMR Chemical Shifts. Isotropic ^{77}Se shielding tensors were calculated for optimized geometries of each species at the PBE0/def2-TZVPP level of theory and transformed to ^{77}Se NMR chemical shifts using the recently derived linear relationship.[30] Depending on the level of calculations, the ^{77}Se chemical shift of monomeric *cis,trans*-$Se(N^tBu)_2$ (conformation **1B**; see Chart 2) has previously been calculated to be 1741[31] or 1696 ppm.[8]

In this contribution, the ^{77}Se chemical shift of the dimer $^tBuNSe(\mu\text{-}N^tBu)_2SeN^tBu$ was calculated for each conformation **2A**−**2E** (see Chart 2). In contrast to our earlier MP2/cc-pVDZ//B3PW91/6-31G* calculations,[3f] in which the all-cis conformation **2A** was found to be the lowest in energy, the present PBE0/def2-TZVPP calculations suggest that the **2D** conformation lies at the lowest energy. However, the other conformations are only a little higher in energy (7.1−12.2 kJ mol^{-1}). The ^{77}Se chemical shifts calculated for the different conformations were as follows: 1294 (**2A**), 1034 (**2B**), 1155 (**2C**), 1348 and 1105 (**2D**), and 1335 and 1130 (**2E**) ppm.

DOI: 10.1021/acs.inorgchem.5b01434
Inorg. Chem. 2015, 54, 9499−9508

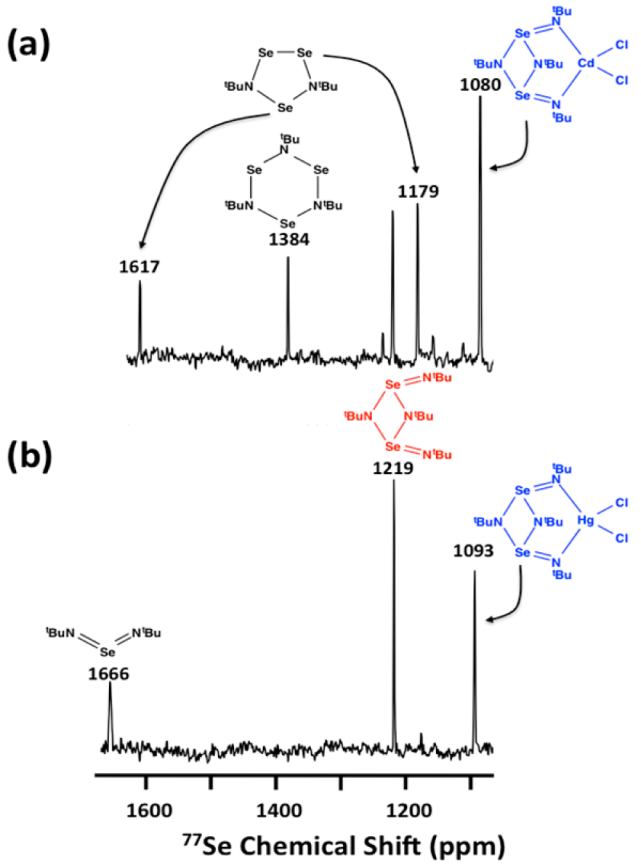

Figure 2. ^{77}Se NMR spectra of crystals of (a) **1**·MeCN and (b) **2**·MeCN redissolved in CH_3CN/CD_3CN.

Because the energy differences between the conformations are small, it is likely that they all are in equilibrium in solution and, consequently, the observed ^{77}Se NMR resonance reflects the calculated average value of 1213 ppm.[32] Although the chemical shifts are computed for species in a vacuum, this value is remarkably close to the chemical shift of 1219 ppm observed in the spectra of both **1** and **2** in CH_3CN/CD_3CN.

Relative Stabilities of Metal Complexes. Two obvious questions need to be considered in light of the results presented above. The first issue concerns the role of the metal center in the cyclodimerization of *tert*-butylselenium diimide because all previously characterized complexes incorporate the monomeric N,N′-chelated $Se(N^tBu)_2$ ligand. The second question involves the stability of the dimer ^{t}BuNSe(μ-N^{t}Bu)$_2$SeN^{t}Bu. The strong resonance assigned to the dimer in CH_3CN/CD_3CN solutions of crystals of **1**·MeCN and **2**·MeCN indicates that it has a significant lifetime in solution. By contrast, there is no evidence for the presence of the dimer in THF or toluene solutions of the monomers $Se(NR)_2$ (R = ^{t}Bu, adamantyl), although several cyclic selenium imides are formed via thermal decomposition.[3e,f] In order to understand the unanticipated cyclodimerization of $Se(N^tBu)_2$ during the formation of the complexes with group 12 dihalogenides, we have carried out PBE0/def2-TZVPP calculations of the energy profile for this process. We have also compared ΔG° for the formation of MCl_2 complexes containing monomeric or dimeric selenium diimide ligands (see Scheme 2) for the species reported in this work (M = Cd, Hg), as well as the known group 10 complexes (M = Pd,[11f] Pt[12]) and the hypothetical complexes (M = Zn, Ni).

Scheme 2. Formation of Complexes Containing *tert*-Butylselenium Diimide Monomer and Dimer (M = Zn, Cd, Hg, Ni, Pd, Pt)

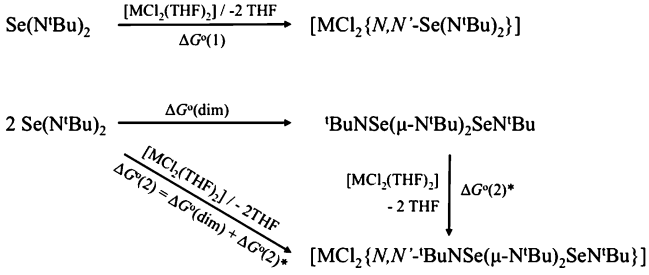

The PBE0/def2-TZVPP calculations give a ΔG° value of +4 kJ mol^{-1} for the cyclodimerization of $Se(N^tBu)_2$ in a vacuum, which can be compared with the value of +7 kJ mol^{-1} obtained for the cyclodimerization of $Se(NMe)_2$ at the CCSD(T)/cc-pVDZ level of theory.[3f] The calculated reaction energies (see Figure 3) predict that the complexes with dimeric ^{t}BuNSe(μ-N^{t}Bu)$_2$SeN^{t}Bu ligands are clearly preferred over those with monomeric ligands for the group 12 metals zinc, cadmium, and mercury, consistent with the experimental findings in this work. The formation of [MCl_2{*N,N*′-^{t}BuNSe(μ-N^{t}Bu)$_2$SeN^{t}Bu}] is generally more favorable than that of [MCl_2{*N,N*′-Se(N^{t}Bu)$_2$}]. In case of group 10 metals, the differences between the Gibbs energies of complexes with the monomeric and dimeric ligands are very small and diminish the group from nickel to platinum (see Figure 3). In fact, platinum shows a preference for coordination with the monomeric ligand, while palladium and nickel have an almost equal propensity for complex formation with either monomeric or dimeric *tert*-butylselenium diimide. In practice, the structurally characterized complexes [MCl_2{*N,N*′-Se(N^{t}Bu)$_2$}] of both palladium (M = Pd[11f]) and platinum (M = Pt[12]) incorporate the monomeric ligand.

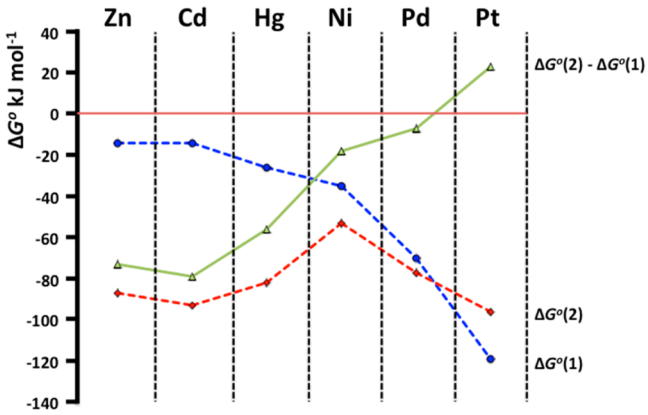

Figure 3. Gibbs energies for the formation of [MCl_2{Se(N^{t}Bu)$_2$}] [ΔG°(**1**)] (blue circles) and [MCl_2{^{t}BuNSe(μ-N^{t}Bu)$_2$SeN^{t}Bu}] [ΔG°(**2**)] (red squares) and their difference (green triangles). The dashed or solid lines connecting the points are only displayed for clarity.

Formation and Stability of ^{t}BuNSe(μ-N^{t}Bu)$_2$SeN^{t}Bu. In order to understand the unprecedented observation of the preferential formation of stable group 12 complexes of the dimer ^{t}BuNSe(μ-N^{t}Bu)$_2$SeN^{t}Bu and to assess the kinetic stability of both monomeric and dimeric selenium diimides, we have investigated the reaction pathway and activation

DOI: 10.1021/acs.inorgchem.5b01434
Inorg. Chem. 2015, 54, 9499−9508

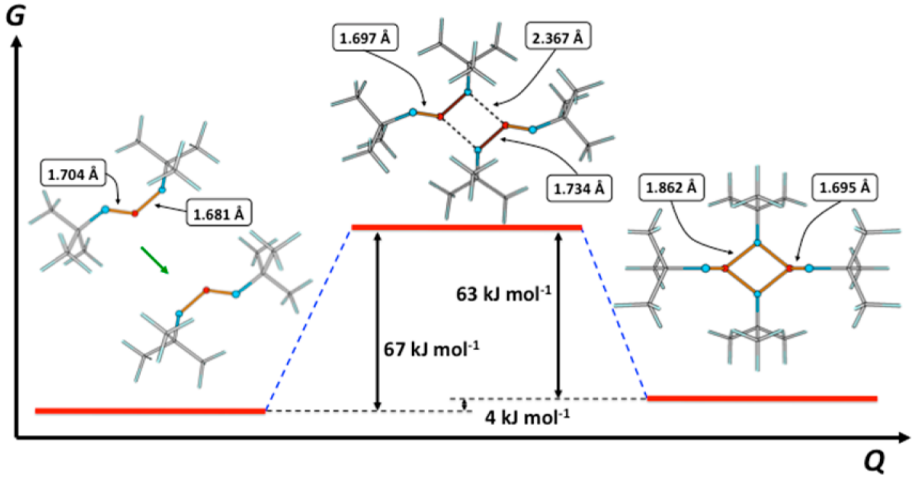

Figure 4. PBE0/def2-TZVPP energetics of the [2 + 2] cyclodimerization of $Se(N^tBu)_2$.

energy of the [2 + 2] cyclodimerization of $Se(N^tBu)_2$. The PBE0/def2-TZVPP reaction profile for this process is shown in Figure 4, together with the optimized geometries of the $Se(N^tBu)_2$ monomer, the ^{t}BuNSe(μ-N^{t}Bu)$_2$SeN^{t}Bu dimer, and the cycloaddition transition state. The transition state exhibits one imaginary frequency and lies 67 kJ mol^{-1} above the selenium diimide monomer and 63 kJ mol^{-1} above the dimer. The values reported in Figure 4 are based on calculations in a vacuum, but the energetics in THF are essentially identical.[33]

As visualized in Figure 3, the differences in the Gibbs energies of the formation of the complexes [MCl_2{^{t}BuNSe(μ-N^{t}Bu)$_2$SeN^{t}Bu}] and [MCl_2{$Se(N^tBu)_2$}] are −74, −79, −56, −18, −7, and +23 kJ mol^{-1} for zinc, cadmium, mercury, nickel, palladium, and platinum, respectively. Thus, the energy difference for nickel and palladium is much smaller than in the case of group 12 metal halogenides. In the case of platinum, the complex with the monomeric ligand is actually more stable than that with the dimer. It is thus understandable that only [MCl_2{$Se(N^tBu)_2$}] has been observed for both palladium and platinum;[11f,12] it is also likely that the nickel complex will contain the monomeric ligand.

In the case of zinc, cadmium, and mercury, the difference in the Gibbs energy between [MCl_2{^{t}BuNSe(μ-N^{t}Bu)$_2$SeN^{t}Bu}] and [MCl_2{$Se(N^tBu)_2$}] is sufficient to initiate and sustain the [2 + 2] cyclodimerization of $Se(N^tBu)_2$, leading to the prediction that $ZnCl_2$ will also form a complex with the dimer. The PBE0/def2-TZVPP reaction profile for the $ZnCl_2$-assisted cyclodimerization of $Se(N^tBu)_2$ is shown in Figure 5. It is likely that $CdCl_2$ and $HgCl_2$ also behave in a similar fashion.

There are two conceivable pathways for the cyclodimerization involving the group 12 metal center, as shown in Figure 5. One pathway is initiated by the formation of the complex [MCl_2{$Se(N^tBu)_2$}] (M = Zn, Cd, Hg) containing the N,N′-chelated monomeric selenium diimide ligand.[34] This complex reacts further with another molecule of $Se(N^tBu)_2$ (arrangement **A**) to form the final complex [MCl_2{^{t}BuNSe(μ-N^{t}Bu)$_2$SeN^{t}Bu}] (**C**) via the transition state **TS1**. It can be seen from Figure 5 that the activation energy for this cyclodimerization process involving zinc chloride is only 21 kJ mol^{-1}, which is significantly lower than that of the cyclodimerization taking place without the presence of the metal chloride (see also Figure 4). It is very likely that the activation barriers in the case of $CdCl_2$ and $HgCl_2$ are of the same order of magnitude. This low activation barrier together

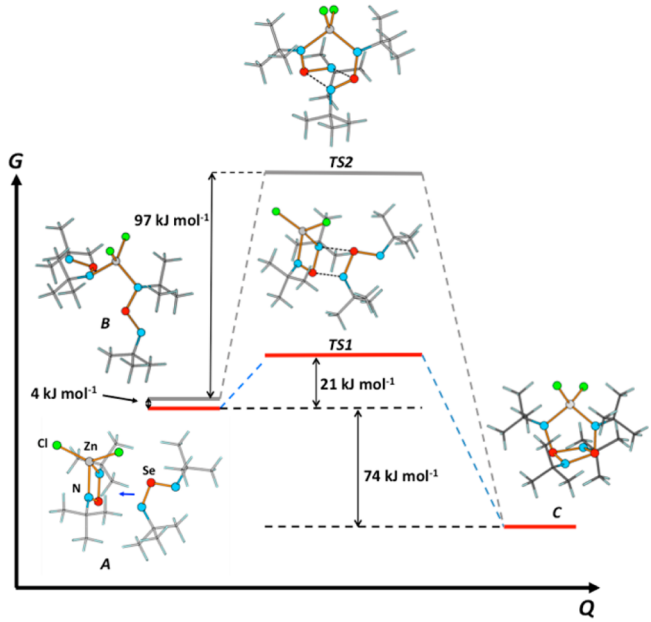

Figure 5. PBE0/def2-TZVPP energetics of two alternative pathways for the $ZnCl_2$-assisted cyclodimerization of $Se(N^tBu)_2$.

with the relatively large Gibbs energy changes of the reaction [ΔG_f° = −74 kJ mol^{-1} in the case of $ZnCl_2$] and provides an explanation for the observation that the cyclodimerization of $Se(N^tBu)_2$ takes place in the presence of group 12 metal chlorides, while the dimer ^{t}BuNSe(μ-N^{t}Bu)$_2$SeN^{t}Bu is not present among the decomposition products of monomeric selenium diimide in solution.

The second alternative reaction pathway involves the initial formation of [MCl_2{*N*-$Se(N^tBu)_2$}$_2$] (**B**) in which two ligands $Se(N^tBu)_2$ show monodentate coordination (see Figure 5). The reorganization of the two ligands (transition state **TS2**) leads to the final complex **C**. While **B** lies only 4 kJ mol^{-1} higher in energy than [MCl_2{$Se(N^tBu)_2$}] + $Se(N^tBu)_2$, the transition state **TS2** lies 97 kJ mol^{-1} higher in energy, rendering this pathway unlikely.

Finally, we note that the high activation energy for the dissociation of ^{t}BuNSe(μ-N^{t}Bu)$_2$SeN^{t}Bu into two monomers combined with the small Gibbs energy of the reaction (see

DOI: 10.1021/acs.inorgchem.5b01434
Inorg. Chem. 2015, 54, 9499−9508

Figure 4) explains the persistent presence of the dimer in acetonitrile solutions of **1** and **2**.

Crystal Structure of 3·4CH$_2$Cl$_2$. In one attempt, the reaction of CdCl$_2$ and Se(N^{t}Bu)$_2$ afforded a minor product, which after recrystallization from CH$_2$Cl$_2$ was identified by a single-crystal X-ray structure determination as the solvated heptanuclear complex **3**·4CH$_2$Cl$_2$ in which selenium(II) diamide ligands are N,N′-chelated to the cadmium centers (see Chart 3).[35]

Chart 3. Heptanuclear Cluster 3

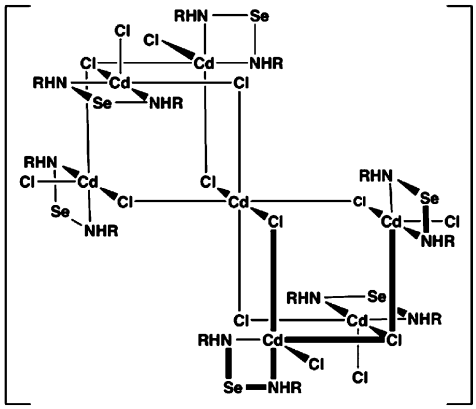

The molecular structure of **3**·4CH$_2$Cl$_2$ indicating the labeling of atoms is shown in Figure 6. The centrosymmetric structure

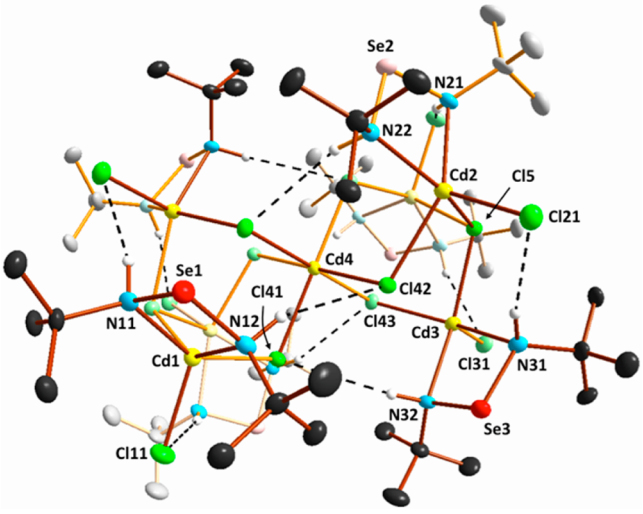

Figure 6. Molecular structure of **3** indicating the numbering of the atoms. The thermal ellipsoids have been drawn at the 50% probability level. Methyl hydrogen atoms and lattice solvent (CH$_2$Cl$_2$) molecules are not shown for clarity. Selected bond parameters are presented in Table 1S in the Supporting Information.

consists of one octahedral cadmium center, which is linked to six square-pyramidal cadmium centers by bridging μ_2-chlorido ligands. The coordination sphere around each of these cadmium centers is completed by one N,N′-chelating selenium diamide Se^{II}(NH^{t}Bu)$_2$ ligand, two terminal chlorido ligands, and one μ_3-chlorido ligand, which bridges two adjacent [CdCl$_2${*N*,*N*′-Se(NH^{t}Bu)$_2$}] moieties. While there are several cadmium complexes that exhibit related structural features, they form extended structures containing mainly octahedral cadmium centers.[37] To our knowledge, **3**·4CH$_2$Cl$_2$ is the first electrically neutral complex containing discrete heptanuclear cadmium environments. The closest structural similarities are found in [Cd$_5$Cl$_{10}$(apda)$_2$]$_n$ [apda = *N*-(2-aminoethyl)-piperazine-1,4-diethylamine][38] and [Li$_2$Cd$_5$Cl$_8$Ar$_4$(THF)$_2$] [Ar = 2,6-(mes)$_2$C$_6$H$_3$].[39]

As expected, the terminal Cd−Cl bonds [2.4226(17)−2.4497(16) Å] are considerably shorter than the bridging Cd−Cl(μ_2) and Cd−Cl(μ_3) bonds, which exhibit values of 2.5807(13)−2.6337(16) and 2.6255(14)-2.6611(16) Å, respectively. The structure of **3** is further stabilized by weak intramolecular NH···Cl contacts, as depicted in Figure 6.

The nitrogen atoms in the Se^{II}(NH^{t}Bu)$_2$ ligands in **3** show tetrahedral geometry with a mean Se−N bond distance of 1.885 Å typical of single bonds.[26] This bond length can be compared to |*d*(Se−N)| = 1.849 Å for Se^{II}(NHMes)$_2$,[8] which is the only other structurally characterized secondary selenium diamide, and to two other diamide derivatives, Se^{II}{N(SiMe$_3$)$_2$}$_2$ (1.869 Å)[40] and Se^{II}{N(^{t}Bu)(SiMe$_3$)}$_2$ (1.863 Å).[41]

CONCLUSIONS

We have described the unprecedented [2 + 2] cyclodimerization of the selenium diimide Se(N^{t}Bu)$_2$ in reactions with group 12 metal dichlorides to give the N,N′-chelated complexes [MCl$_2${*N*,*N*′-^{t}BuNSe(μ-N^{t}Bu)$_2$SeN^{t}Bu}] [M = Cd (**1**), Hg (**2**)]. PBE0/def2-TZVPP calculations have assisted in the assignment of the ^{77}Se NMR resonance for the novel dimer ^{t}BuNSe(μ-N^{t}Bu)$_2$SeN^{t}Bu, which is formed in solutions of recrystallized **1** and **2** in acetonitrile. Consistent with the experimental observations, the computed energetics of the reactions of Se(N^{t}Bu)$_2$ with MCl$_2$ (M = Zn, Cd, Hg, Ni, Pd, Pt) reveal that complexes of ^{t}BuNSe(μ-N^{t}Bu)$_2$SeN^{t}Bu are more stable for the group 12 metals than those containing the monomeric ligand. Furthermore, DFT calculations indicate that the activation energy for the cyclodimerization process is significantly lower in the presence of group 12 metal chlorides than in the absence of the chloride. The high activation barrier for the [2 + 2] cyclodimerization of Se(N^{t}Bu)$_2$ explains the following experimental observations: (a) the kinetic stability and persistence of the dimer ^{t}BuNSe(μ-N^{t}Bu)$_2$SeN^{t}Bu once it is formed in solution and (b) the absence of dimer formation in the preparation and subsequent decomposition of selenium diimides. It is yet to be established whether the prevalence of metal complexes of dimeric selenium diimide ligands is restricted to group 12 metals or is a more general phenomenon.

ASSOCIATED CONTENT

Supporting Information

The Supporting Information is available free of charge on the ACS Publications website at DOI: 10.1021/acs.inorgchem.5b01434.

Selected bond parameters of **3**·4CH$_2$Cl$_2$, geometry optimization of [MCl$_2${Se$_n$(N^{t}Bu)$_{2n}$}] (n = 1, 2), PBE0/SVP energy profile of the formation of [ZnCl$_2${*N*,*N*′-Se(N^{t}Bu)$_2$}] from [MCl$_2$(THF)$_2$] and Se(N^{t}Bu)$_2$, and Cartesian coordinates of the PBE0/def2-TZVPP-optimized geometries (PDF)

X-ray crystallographic file in CIF format of **1**·MeCN (CIF)

X-ray crystallographic file in CIF format of **2**·MeCN (CIF)

DOI: 10.1021/acs.inorgchem.5b01434
Inorg. Chem. 2015, 54, 9499−9508

X-ray crystallographic file in CIF format of $3{\cdot}4CH_2Cl_2$ (CIF)

AUTHOR INFORMATION

Corresponding Author

*Phone: +358294 481611. E-mail: risto.laitinen@oulu.fi.

Notes

The authors declare no competing financial interest.

ACKNOWLEDGMENTS

Financial support from the Academy of Finland [Grants 134548 (to R.S.L.) and 253400 (to J.M.R.)], Finnish Cultural Foundation (to A.J.K.), and Magnus Ehrnrooth Foundation (to A.J.K.), as well as from NSERC (Canada; to T.C.) is gratefully acknowledged. We are also grateful to Finnish CSC, IT for Science Ltd., for their generous provision of computational resources.

REFERENCES

(1) (a) Chivers, T. *A Guide to Chalcogen-Nitrogen Chemistry*; World Scientific Publishing Co. Pte. Ltd.: Singapore, 2005. (b) Chivers, T.; Laitinen, R. S. Chalcogen−Nitrogen Chemistry. In *Handbook of Chalcogen Chemistry, New Perspectives in Sulfur, Selenium and Tellurium*; Devillanova, F., Ed.; RSC Press: Cambridge, U.K., 2007; pp 223−285. (c) Laitinen, R. S.; Oilunkaniemi, R.; Chivers, T. Synthesis, Structures, Bonding, and Reactions of Imido-Selenium and -Tellurium Compounds. In *Selenium and Tellurium Chemistry: From Small Molecules to Biomolecules and Materials*; Woollins, J. D., Laitinen, R. S., Eds.; Springer Verlag: Berlin, 2011; pp 103−122. (d) Chivers, T.; Laitinen, R. S. Recent Developments in Chalcogen-Nitrogen Chemistry. In *Handbook of Chalcogen Chemistry: New Perspectives in Sulfur, Selenium and Tellurium*; Devillanova, F., du Mont, W.-W., Eds.; RSC Publishing: Cambridge, U.K., 2013; pp 191−237. (e) Chivers, T.; Laitinen, R. S. *Chem. Soc. Rev.* **2015**, *44*, 1725−1739.

(2) Stalke, D. *Chem. Commun.* **2012**, *48*, 9559−9573 and references cited therein.

(3) (a) Sharpless, K. B.; Hori, T.; Truesdale, L. K.; Dietrich, C. O. *J. Am. Chem. Soc.* **1976**, *98*, 269−271. (b) Herberhold, M.; Jellen, W. *Z. Naturforsch., B: J. Chem. Sci.* **1986**, *41*, 144−148. (c) Fockenberg, F.; Haas, A. *Z. Naturforsch., B: J. Chem. Sci.* **1986**, *41*, 413−422. (d) Wrackmeyer, B.; Distler, B.; Gerstmann, S.; Herberhold, M. *Z. Naturforsch., B: J. Chem. Sci.* **1993**, *48*, 1307−1314. (e) Maaninen, T.; Chivers, T.; Laitinen, R.; Schatte, G.; Nissinen, M. *Inorg. Chem.* **2000**, *39*, 5341−5347. (f) Maaninen, T.; Tuononen, H. M.; Schatte, G.; Suontamo, R.; Valkonen, J.; Laitinen, R.; Chivers, T. *Inorg. Chem.* **2004**, *43*, 2097−2104.

(4) (a) Chivers, T.; Gao, X.; Parvez, M. *J. Chem. Soc., Chem. Commun.* **1994**, 2149−2150. (b) Chivers, T.; Gao, X.; Parvez, M. *J. Am. Chem. Soc.* **1995**, *117*, 2359−2360. (c) Chivers, T.; Gao, X.; Parvez, M. *Inorg. Chem.* **1996**, *35*, 9−15. (d) Chivers, T.; Sandblom, N.; Schatte, G. *Inorg. Synth.* **2004**, *34*, 42−48.

(5) (a) Herberhold, M.; Distler, B.; Maisel, H.; Milius, W.; Wrackmeyer, B.; Zanello, P. *Z. Anorg. Allg. Chem.* **1996**, *622*, 1515−1523. (b) Christe, K. O.; Gerken, M.; Haiges, R.; Schneider, S.; Schroer, T.; Tham, F. S.; Vij, A. *Solid State Sci.* **2002**, *4*, 1529−1534. (c) Maaninen, T.; Laitinen, R.; Chivers, T. *Chem. Commun.* **2002**, 1812−1813. (d) Schatte, G.; Chivers, T.; Tuononen, H. M.; Suontamo, R.; Laitinen, R.; Valkonen, J. *Inorg. Chem.* **2005**, *44*, 443−451.

(6) Sandblom, N.; Ziegler, T.; Chivers, T. *Inorg. Chem.* **1998**, *37*, 354−359.

(7) Tuononen, H. M.; Suontamo, R. J.; Valkonen, J. U.; Laitinen, R. S.; Chivers, T. *Inorg. Chem.* **2003**, *42*, 2447−2454.

(8) Maaninen, T.; Tuononen, H. M.; Kosunen, K.; Oilunkaniemi, R.; Hiitola, J.; Laitinen, R.; Chivers, T. *Z. Anorg. Allg. Chem.* **2004**, *630*, 1947−1954.

(9) Bestari, K.; Cordes, A. W.; Oakley, R. T.; Young, K. M. *J. Am. Chem. Soc.* **1990**, *112*, 2249−2255.

(10) Hill, A. F. *Adv. Organomet. Chem.* **1994**, *36*, 159−227.

(11) (a) Kops, R. T.; Van Aken, E.; Schenk, H. *Acta Crystallogr., Sect. B: Struct. Crystallogr. Cryst. Chem.* **1973**, *29*, 913−914. (b) Meij, R.; Olie, K. *Cryst. Struct. Commun.* **1975**, *4*, 515−520. (c) Mahabiersing, C.; de Lange, W. G. J.; Goubitz, K.; Stufkens, D. J. *J. Organomet. Chem.* **1993**, *461*, 127−139. (d) Roesky, H. W.; Schmidt, H.-G.; Noltemeyer, M.; Sheldrick, G. M. *Chem. Ber.* **1983**, *116*, 1411−1414. (e) Gindl, J.; Björgvinsson, M.; Roesky, H. W.; Freire-Erdbrügger, C.; Sheldrick, G. M. *J. Chem. Soc., Dalton Trans.* **1993**, 811−812. (f) Risto, M.; Eironen, A.; Männistö, E.; Oilunkaniemi, R.; Laitinen, R. S.; Chivers, T. *Dalton Trans.* **2009**, 8473−8475.

(12) Karhu, A. J.; Risto, M.; Rautiainen, M. J.; Oilunkaniemi, R.; Chivers, T.; Laitinen, R. S. 2015, to be published.

(13) Risto, M.; Takaluoma, T. T.; Bajorek, T.; Oilunkaniemi, R.; Laitinen, R. S.; Chivers, T. *Inorg. Chem.* **2009**, *48*, 6271−6279.

(14) (a) Chivers, T.; Parvez, M.; Schatte, G. *Angew. Chem., Int. Ed.* **1999**, *38*, 2217−2219. (b) Chivers, T.; Parvez, M.; Schatte, G. *Inorg. Chem.* **1999**, *38*, 5171−5177.

(15) Risto, M.; Konu, J.; Oilunkaniemi, R.; Laitinen, R. S.; Chivers, T. *Polyhedron* **2010**, *29*, 871−875.

(16) Chivers, T.; Schatte, G. *Can. J. Chem.* **2003**, *81*, 1307−1314.

(17) Burns, R. C.; Collins, M. J.; Gillespie, R. J.; Schrobilgen, G. J. *Inorg. Chem.* **1986**, *25*, 4465−4469.

(18) Sens, M. A.; Wilson, N. K.; Ellis, P. D.; Odom, J. D. *J. Magn. Reson.* **1975**, *19*, 323−336.

(19) Sheldrick, G. M. *Acta Crystallogr., Sect. A: Found. Crystallogr.* **2008**, *64*, 112−122.

(20) Frisch, M. J.; Trucks, G. W.; Schlegel, H. B.; Scuseria, G. E.; Robb, M. A.; Cheeseman, J. R.; Scalmani, G.; Barone, V.; Mennucci, B.; Petersson, G. A.; Nakatsuji, H.; Caricato, M.; Li, X.; Hratchian, H. P.; Izmaylov, A. F.; Bloino, J.; Zheng, G.; Sonnenberg, J. L.; Hada, M.; Ehara, M.; Toyota, K.; Fukuda, R.; Hasegawa, J.; Ishida, M.; Nakajima, T.; Honda, Y.; Kitao, O.; Nakai, H.; Vreven, T.; Montgomery, J. A., Jr.; Peralta, J. E.; Ogliaro, F.; Bearpark, M.; Heyd, J. J.; Brothers, E.; Kudin, K. N.; Staroverov, V. N.; Kobayashi, R.; Normand, J.; Raghavachari, K.; Rendell, A.; Burant, J. C.; Iyengar, S. S.; Tomasi, J.; Cossi, M.; Rega, N.; Millam, M. J.; Klene, M.; Knox, J. E.; Cross, J. B.; Bakken, V.; Adamo, C.; Jaramillo, J.; Gomperts, R.; Stratmann, R. E.; Yazyev, O.; Austin, A. J.; Cammi, R.; Pomelli, C.; Ochterski, J. W.; Martin, R. L.; Morokuma, K.; Zakrzewski, V. G.; Voth, G. A.; Salvador, P.; Dannenberg, J. J.; Dapprich, S.; Daniels, A. D.; Farkas, Ö.; Foresman, J. B.; Ortiz, J. V.; Cioslowski, J.; Fox, D. J. *Gaussian 09*, revision D.01; Gaussian, Inc.: Wallingford, CT, 2013.

(21) (a) Perdew, J. P.; Burke, K.; Ernzerhof, M. *Phys. Rev. Lett.* **1996**, *77*, 3865−3868. (b) Perdew, J. P.; Burke, K.; Ernzerhof, M. *Phys. Rev. Lett.* **1997**, *78*, 1396. (c) Perdew, J. P.; Ernzerhof, M.; Burke, K. *J. Chem. Phys.* **1996**, *105*, 9982−9985. (d) Adamo, C.; Barone, V. *J. Chem. Phys.* **1999**, *110*, 6158−6170.

(22) (a) Weigend, F.; Ahlrichs, R. *Phys. Chem. Chem. Phys.* **2005**, *7*, 3297−3305. (b) Andrae, D.; Häußermann, U.; Dolg, M.; Stoll, H.; Preuß, H. *Theor. Chim. Acta* **1990**, *77*, 123−141.

(23) Grimme, S.; Ehrlich, S.; Goerigk, L. *J. Comput. Chem.* **2011**, *32*, 1456−1465.

(24) (a) Barone, V.; Cossi, M. *J. Phys. Chem. A* **1998**, *102*, 1995−2001. (b) Cossi, M.; Rega, N.; Scalmani, G.; Barone, V. *J. Comput. Chem.* **2003**, *24*, 669−681.

(25) (a) McWeeny, R. *Phys. Rev.* **1962**, *126*, 1028−1034. (b) Ditchfield, R. *Mol. Phys.* **1974**, *27*, 789−807. (c) Wolinski, K.; Hinton, J. F.; Pulay, P. *J. Am. Chem. Soc.* **1990**, *112*, 8251−8260. (d) Cheeseman, J. R.; Trucks, G. W.; Keith, T. A.; Frisch, M. J. *J. Chem. Phys.* **1996**, *104*, 5497−5509.

(26) Emsley, J. *The Elements*, 3rd ed.; Clarendon Press: Oxford, U.K., 1998.

(27) It has been deduced by McFarlane and McFarlane that the relationship between the ^{125}Te and ^{77}Se chemical shifts is generally $\delta(^{125}\text{Te}) \sim 1.8\delta(^{77}\text{Se})$,[28] although significantly smaller ratios spanning 0.4−1.6 have also been reported.[29]

DOI: 10.1021/acs.inorgchem.5b01434
Inorg. Chem. 2015, 54, 9499−9508

(28) McFarlane, H. C. E.; McFarlane, W. *J. Chem. Soc., Dalton Trans.* **1973**, 2416−2418.
(29) Risto, M.; Jahr, E. M.; Hannu-Kuure, M. S.; Oilunkaniemi, R.; Laitinen, R. S. *J. Organomet. Chem.* **2007**, *692*, 2193−2204 and references cited therein.
(30) $\delta(^{77}\mathrm{Se}) = 1945.5 - 1.05\sigma_{iso}$.[31]
(31) Karhu, A. J.; Pakkanen, O. J.; Rautiainen, J. M.; Oilunkaniemi, R.; Chivers, T.; Laitinen, R. S. *Inorg. Chem.* **2015**, *54*, 4990−4997.
(32) The relative concentrations of the different conformations have been estimated using the Boltzmann distribution by taking their relative energies into account. The observed chemical shift is assumed to be the concentration-weighted average of the chemical shifts of individual conformations. The simple average of the individual chemical shifts of the different conformations is 1200 ppm, which also supports the current assignment.
(33) The PBE0/def2-TZVPP energetics in THF show that the Gibbs energy of the [2 + 2] cyclodimerization of $Se(N^tBu)_2$ is 3 kJ mol^{-1} and the activation energy is 73 kJ mol^{-1}. The activation energy for the dissociation of the dimer ^{t}BuNSe(μ-N^{t}Bu)$_2$SeN^{t}Bu is 70 kJ mol^{-1}.
(34) Preliminary computation of the energy profile of the formation of [$ZnCl_2${*N*,*N*′-$Se(N^tBu)_2$}] from [$ZnCl_2(THF)_2$] and $Se(N^tBu)_2$ could only be carried out at the PBE0/SVP level of theory and is shown in the Supporting Information. The highest activation energy was calculated to be 30 kJ mol^{-1}, and the Gibbs energy change in the total process is almost energy neutral of +9 kJ mol^{-1}. The energy values, however, are dependent on the level of the theory. At the PBE0/def2-TZVPP level of theory, the total Gibbs energy change in the formation of [$ZnCl_2${*N*,*N*′-$Se(N^tBu)_2$}] from [$ZnCl_2(THF)_2$] and $Se(N^tBu)_2$ is −14 kJ mol^{-1} (see Figure 3).
(35) The source of $Se^{II}(NH^tBu)_2$ is unknown, but it may have been present as a minor impurity in some batches of $Se(N^tBu)_2$, which showed an unidentified ^{77}Se NMR resonance at 925 ppm, compared to 974 ppm for $Se^{II}(NMe_2)_2$.[36] We have previously observed that the attempted preparation of $Se^{IV}\{N(mes)\}_2$ (mes = mesityl) by the reaction of (mes)NHLi and $SeCl_4$ produced $Se^{II}(NH\{mes\})_2$ according to the following equation:[8]

$$4(mes)NHLi + SeCl_4 \rightarrow Se\{NH(mes)\}_2 + \frac{1}{2}(mes)N{=}{=}N(mes) + (mes)NH_2 + 4LiCl$$

(36) King, R. B.; Sangokoya, S. A. *Inorg. Chem.* **1987**, *26*, 2727−2730.
(37) *ConQuest*, version 1.17; Cambridge Crystallographic Data Center, Cambridge, U.K., 2015.
(38) Satapathi, S.; Choubey, S.; Bhar, K.; Chattopadhyay, S.; Mitra, P.; Slawin, A. M. Z.; Ghosh, B. K. *Inorg. Chim. Acta* **2012**, *384*, 37−46.
(39) Gridley, B. M.; Blundell, T. J.; Moxey, G. J.; Lewis, W.; Blake, A. J.; Kays, D. L. *Chem. Commun.* **2013**, *49*, 9752−9754.
(40) Björgvinsson, M.; Roesky, H. W.; Pauer, F.; Stalke, D.; Sheldrick, G. M. *Inorg. Chem.* **1990**, *29*, 5140−5143.
(41) Björgvinsson, M.; Roesky, H. W.; Pauer, F.; Stalke, D.; Sheldrick, G. M. *Eur. J. Solid State Inorg. Chem.* **1992**, *29*, 759−776.

DOI: 10.1021/acs.inorgchem.5b01434
Inorg. Chem. 2015, 54, 9499−9508